Food Chemistry 250 (2018) 75–82

Contents lists available at ScienceDirect

Food Chemistry

journal homepage: www.elsevier.com/locate/foodchem

Impact of *Prosopis alba* exudate gum on sorption properties and physical stability of fish oil alginate beads prepared by ionic gelation

Franco Emanuel Vasile[a,c,*], María Alicia Judis[a], María Florencia Mazzobre[b,c]

[a] Laboratorio de Industrias Alimentarias II, Universidad Nacional del Chaco Austral, Comandante Fernández 755, Presidencia Roque Sáenz Peña 3700, Chaco, Argentina
[b] Laboratorio de Conservación de Biomoléculas, Departamento de Industrias, Facultad de Ciencias Exactas y Naturales, Universidad de Buenos Aires, Ciudad Universitaria-Pabellón Industrias (1428), Buenos Aires, Argentina
[c] Consejo Nacional de Investigaciones Científicas y Técnicas (CONICET), Argentina

ARTICLE INFO

Chemical compounds studied in this article:
Sodium alginate (PubChem CID: 5102882)
Chitosan (PubChem CID: 71853)
Calcium chloride (PubChem CID: 5284359)
Chloroform (PubChem CID: 6212)
Methanol (PubChem CID: 887)
Ammonium thiocyanate (PubChem CID: 15666)
Iron (II) chloride (PubChem CID: 24458)

Keywords:
*Prosopis alba*exudate gum
Ionic gelation
Glass transition
Oxidative stability
Optical properties

ABSTRACT

This study was conducted to evaluate the effect of *Prosopis alba* exudate gum (G) as encapsulating matrix component on water-solid interactions, physical state, oxidative damage and appearance properties of alginate-chitosan encapsulates containing fish oil. With this purpose, water sorption isotherms were obtained at 25 °C. G increased the hygroscopicity of encapsulates, showing a higher monolayer water content (7.87 ± 0.47% db.) than control (1.07 ± 0.04% db.). G introduction reduced the plasticizing effect of water, increasing the a_w range (a_w < 0.45) at which samples were in amorphous state and providing the highest protection against lipid oxidation. Appearance properties (chromatic and optical) were affected by hydration and were better maintained in samples containing G at a_w > 0.52. These results allow considering *Prosopis alba* exudate gum, as a novel excipient to protect fish oil encapsulated in low moisture polyelectrolyte systems, with the added benefits of employing an undervalued natural resource.

1. Introduction

The protection of bioactive oils from oxidative damage, has focused the scientist's attention on the development of innovative strategies. Encapsulation and nano-encapsulation of functional oils arises in the last years as a novel and practical technology (Ghorbanzade, Jafari, Akhavan, & Hadavi, 2017; Pourashouri et al., 2014; Rodríguez, Martín, Ruiz, & Clares, 2016). Many encapsulation methods were developed in order to transform oils into easily-handled powdery solids and to protect them from oxidation through a solid wall acting as a physical barrier to oxygen diffusion (Rodríguez et al., 2016). Particularly, ionic gelation has been recently proposed for the entrapment and protection of easily oxidized lipids as essentials oils (Benavides, Cortés, Parada, & Franco, 2016; Mokhtari, Jafari, & Assadpour, 2017) and oils rich in polyunsaturated fatty acids (Vasile, Romero, Judis, & Mazzobre, 2016).

Ionic gelation is based on the crosslinking of polyelectrolyte chains, generally alginate, in the presence of divalent cations such as calcium. Calcium ions form junction zones between carboxylates groups of alginate molecules forming an open lattice structure gel able to entrap bioactive compounds. The obtained encapsulates could be used in hydrated form (hydrogels), or dehydrated. During dehydration, water removal leads to an amorphous glassy matrix with a disordered structure of high and low molecular weight compounds (Augustin, Sanguansri, Decker, Elias, & McClements, 2010). The immobilization procedure on alginate beads is not only inexpensive but also very easy to carry out and provides extremely mild conditions, so that the potential for industrial application is considerable (Li & Li, 2010; Mokhtari et al., 2017). However, some disadvantages such as low mechanical strength, large pore size, erosion and low retention capacity, among other issues have conducted to modify the alginate-calcium basic system (Elnashar, Danial, & Awad, 2009). The most frequent approaches have been focused on the use of alginate in combination with others hydrocolloids such as whey (Aguilar et al., 2015), chitosan, pectin (Wang, Waterhouse, & Sun-Waterhouse, 2013), cornstarch, and other gums capable of forming composite or multilayer structures that allow to improve retention capacity, yield and encapsulation efficiency. Several physicochemical properties of encapsulates as hygroscopicity and structural stability could be strongly affected by the inclusion of

* Corresponding author at: Comandante Fernández 755, Presidencia Roque Sáenz Peña (3700), Chaco, Argentina.
E-mail addresses: francovasile@uncaus.edu.ar (F.E. Vasile), judis@uncaus.edu.ar (M.A. Judis), florm@di.fcen.uba.ar (M.F. Mazzobre).

https://doi.org/10.1016/j.foodchem.2018.01.018
Received 30 June 2017; Received in revised form 31 December 2017; Accepted 2 January 2018
Available online 02 January 2018
0308-8146/

these biopolymers. Considering the high influence of water on stability of dehydrated formulations containing active compounds, the analysis of the solid-water interactions becomes of fundamental importance to define the appropriate processing and storage conditions.

The thermodynamics analysis of water sorption and its relation with structural features in dried encapsulated or microencapsulated oils has drawn interest since it is well known that oxidative stability is greatly influenced by water adsorption, molecular mobility and structural integrity of encapsulated products (Beristain, Azuara, & Vernon-Carter, 2002; Botrel, de Barros Fernandes, Borges, & Yoshida, 2014; Velasco, Holgado, Dobarganes, & Márquez-Ruiz, 2009). Below T_g, lipids compounds are trapped and protected in an amorphous glassy matrix where diffusion-controlled reactions, such as oxidation, are claimed to be kinetically limited. In previous works we purposed the introduction of *Prosopis alba* exudate gum as a novel excipient for alginate-chitosan beads formulations (Vasile, Judis, & Mazzobre, 2017; Vasile et al., 2016). The use of this gum as wall compound allowed enhancing the yield, efficiency, and oxidative stability of a polyunsaturated fish oil of interest. We hypothesize that *P. alba* gum in alginate-chitosan beads, exerts a positive effect on water/solid interactions, physical and oil stability. The objective of present work was to evaluate the effect of *P. alba* gum on sorption properties and physical stability of alginate-chitosan beads. Particularly, changes in water-solid interactions, physical state and appearance properties of the beads containing the gum were studied in relation to the encapsulated oil stability. These studies aim to contribute with scientific and practical bases to the use of a currently wasted gum as a novel functional ingredient for low, medium or high moisture content food products.

2. Materials and methods

2.1. Materials

Prosopis alba exudate gum (G) was obtained by purification of exudates manually collected from trees located in the central zone of the province of Chaco, in the north east region of Argentina. The trees, popularly known as “Algarrobo blanco”, were botanically identified by the IBONE (Botanical Institute of the Northeast, Corrientes, Argentina). The samples included natural exudations (on the main trunk and branches) and also exudations produced by mechanical damages (due to agricultural practices and other types of wounds). The samples had a bitter taste, slightly sweet odor and variable colors (from clear amber to dark reddish brown). The collected exudates were dispersed in water (20% w/v) at 75 °C under constant stirring for 1 h. The suspension was clarified by filtration (Whatman No. 4, Uppsala Sweden) and the resultant solution was frozen at −40 °C and freeze-dried (Rificor, Model L-I-E300-CRT, Buenos Aires, Argentina). Commercial sodium alginate (A) was provided by Cargill (Buenos Aires, Argentina) (Algogel 6020, medium molecular weight 135 kDa, guluronic/mannuronic ratio 56/44). Chitosan (Ch) (medium molecular weight, 190–310 kDa with deacetylation degree of 75–85%) used in this study was purchased from Sigma–Aldrich (St Louis, MO, USA). Refined fish oil (FO) was cordially provided by GHION (Mar del Plata, Argentina) and it was used as supplied. All other reactants were commercially available and used as received. Double distilled water was used in all experiments.

2.2. Methods

2.2.1. Fish oil emulsion and encapsulation process

Sodium alginate (A) and purified *Prosopis alba* exudate gum (G) were dispersed in double distilled water to obtain A and A-G solutions. Both solutions were left standing overnight at room temperature to complete biopolymer hydration. Each batch emulsion (10 g) was formulated with a 1:9 ratio of dispersed oil phase to continuous phase (A or A-G). Emulsion containing alginate had the following composition: fish oil 10% w/w, alginate 1% w/w and water 89% w/w. In 10 g of A emulsion, the content of non-aqueous components was 1.1 g, with an oil:wall material ratio of 10:1. Emulsion containing alginate and *P. alba* exudate gum in a ratio of 1:2, had the following composition: fish oil 10% w/w, alginate 1% w/w, gum 2% w/w, water 87% w/w. In 10 g of A-G emulsion, the content of non-aqueous components was 1.3 g, reaching an oil to wall material ratio of 10:3.

Emulsions composition was established based on previously obtained results (Vasile et al., 2017). Pre-emulsion was obtained by medium-speed homogenization for 2 min using an Ultra-turrax (IKA, Model T18, Staufen, Germany). Emulsion was carried out at 20,000 rpm for 3 min. Then, each emulsion was immersed into an ultrasonic bath (Testlab, Model TB010, Buenos Aires, Argentina) for 3 min. A peristaltic pump (Boading Longer Precision Pump Co, Model BT50-1J, Habei, China) fitted at 9 ± 0.1 rpm, was used to drop the emulsion into a $CaCl_2$ (Cicarelli, p.a.) aqueous solution (20 g/l). The tip of the needle (0.25 mm of inner diameter) was fixed at 6 cm above the surface of the crosslinking solution. The gelling bath was gently stirred with a shaker to prevent beads agglomeration. After generation, the beads were hardened 10 min in the $CaCl_2$ solution and then transferred into a 2% w/v chitosan (Ch) solution (prepared in 0.1 M HCl) for others 10 min. Finally, beads were washed with $CaCl_2$ solution and vacuum dried at 30 °C during 24 h in an oven operating at a chamber pressure of 700 mbar (Fistreem International, Ltd., Loughborough, England) with dried silica gel as desiccant agent.

2.2.2. Water sorption isotherms

Water sorption isotherms of dried beads containing fish oil were determined by the gravimetric static method at 25 °C. Approximately, 100 mg of each system was placed in glass vials with the same size and transparency. Vials were set in separate hermetic chambers containing oversaturated salt solutions in the range from 0.11 to 0.95 of water activity according to reported by Greenspan (1977). The chambers were kept in a temperature-controlled room at 25 °C in the dark. Samples weight were periodically monitored until to reach the equilibrium (± 0.001 g). The equilibrium was reached after approximately thirty days, when the a_w of the samples was equal to the equilibrium relative humidity of the correspondent saturated salt solution in the chamber (Greenspan, 1977). The equilibrium water content was determined by drying at 105 °C until constant weight. Additionally, water sorption isotherms of beads without oil were determined in order to evaluate the influence of the oil in the samples sorption behavior. Oil-free capsules were prepared following the above described method but employing suspension of A and A-G (without the oil) and covered with the chitosan layer.

The sorption data was fitted to BET model (Brunauer, Emmett, & Teller, 1938) defined as:

$$M_e = \frac{M_o C a_w}{[(1-a_w) + (C-1)(1-a_w)a_w]} \quad (1)$$

where M_e is the equilibrium moisture content (% dry basis, db.); M_o is the monolayer water content (% db.); C is an energy constant, related to the difference of free enthalpy (standard chemical potential) of the sorbate molecules in the pure liquid state and in the monolayer, and a_w is the water activity.

The suitability of the model was assessed using the determination coefficient (R^2), the standard error of estimate (SEE), and the mean relative deviation modulus (E). The SEE, indicates the fitting ability of a model to a data set. The lower SEE value, the better is the fitting model ability. SEE is defined as:

$$SEE = \sqrt{\frac{\sum (M_i - M_{Ei})^2}{df}} \quad (2)$$

where M_i is the moisture content at i observation (% db.); M_{Ei} is the predicted moisture content at the same observation, df is the degree of freedom (number of data points minus number of constants in the

model). Furthermore, the mean relative deviation modulus (E) is defined as:

$$E = \frac{100\%}{n} \sum \frac{|M_i - M_{Ei}|}{M_i} \quad (3)$$

where n is the number of observations. It is generally assumed that an E value below 5% is indicative of a good fit for practical applications.

2.2.3. Evaluation of glass transition temperature and plasticizing water effect

The glass transition temperature was determined using a differential scanning calorimetry (DSC) system (Mettler TA 4000, Columbus, Ohio, USA) with TC11 TA processor and GraphWare TA72 thermal analysis software). The instrument was calibrated for temperature, heat flow and enthalpy of melting using triply distilled water (m.p. 0.0 °C, $\Delta H = 6.013\ kJ\ mol^{-1}$), indium (m.p. 156.6 °C, $\Delta H = 3.28\ kJ\ mol^{-1}$), lead (m.p. 327.5 °C, $\Delta H = 4.799\ kJ\ mol - 1$) and zinc (m.p. 419.6 °C, $\Delta H = 7.32\ kJ\ mol^{-1}$). Analysis involved 40 µL aluminium pans (Mettler) containing 5–10 mg samples, hermetically sealed. An empty pan was used as reference. Each sample was heated at a rate of $10\ °C\ min^{-1}$ from −100 to 25 °C (dynamic method). Glass transition temperature was determined as the onset point of the step change on the heat flow curve as described in Mazzobre, Buera, and Chirife (1997).

Experimental T_g-water content (% db.) data was fitted to the Gordon and Taylor (1952) model, considering the onset temperature of the transition:

$$T_{gmix} = \frac{w_s T_{gs} + k_{GT} w_w T_{gw}}{w_s + k_{GT} w_w} \quad (4)$$

where w_s is the solid mass fraction, w_w is the water mass fraction, T_{gs} is the anhydrous-solid glass transition temperature and T_{gw} is the amorphous-water glass transition temperature (−135 °C) (Chen, Fowler, & Toner, 2000), T_{gmix} is the glass transition temperature of the system and k_{GT} is the Gordon and Taylor constant.

2.2.4. Evaluation of lipid oxidation in equilibrated samples

Lipid oxidation was evaluated on the samples equilibrated at different a_w in the previously described storage conditions for approximately at thirty days. The same amount of beads was placed in open glass vials (of same size and transparency), being the head space, exposed surface area and other conditions affecting lipid oxidation, uniform among all treatments. The oil extraction from polyelectrolyte beads was performed by a modification of Bligh and Dyer method according to described in Vasile, Martinez, Pizones Ruiz-Henestrosa, Judis, and Mazzobre (2016). Oxidation degree of samples was monitored spectrophotometrically by means of quantification of primary oxidation products in therms of hydroperoxides concentration. With this purpose, an Evolution 600 UV–Vis Spectrophotometer (Thermo scientific, Waltham, USA) was used. Peroxide value (PV) determination was determined according to the official method developed by IDF (1991), with minor modifications. Briefly, 0.02 ml of extracted oil was dissolved in 9.9 ml of a mixture of chloroform–methanol (70:30) and 0.05 ml of ammonium thiocyanate (0.3 g/ml) were added and spectrophotometrically measured by absorbance at 501 nm to obtain E_0. Then, 0.05 ml of iron (II) chloride solution (0.35 g of iron (II) chloride tetrahydrate in 100 ml of water and 2 ml HCl 10 M) was added and after 5 min of reaction time, absorbance of the red iron (III) complex was determined (E_2). The results were expressed as milliequivalents of oxygen per kilogram of extracted fish oil, according to:

$$PV = \frac{[E_2 - (E_0 + E_1)]}{55.84 * m_o} \quad (5)$$

where E_0 is the absorbance at 501 nm of the reaction mixture before iron (II) chloride solution addition. E_2 is the absorbance at 501 nm after 5 min of iron (II) chloride solution addition. E_1 is the absorbance at 501 nm of reagent blank, and m_o is the mass (g) of the tested oil portion.

2.2.5. Appearance attributes by digital image analysis

Chromatic and optical properties of at least 30 capsules of each formulation were determined by digital image analysis using a computer vision system. Samples were set on glass plates, over white and black backgrounds, and illuminated by a D65 lamp inside a grey chamber ($L^* = 50$ in the CIELAB scale). A high-resolution (3.2 megapixel, 3.0× zoom) digital camera, Canon Power Shot A70 (Canon Inc., Malaysia) equipped with a binocular lens (7× zoom) (Unitron MS, Unitron Inc., NY, USA) was used for the image acquisition. The camera was set at 45° over the object plane at 40 cm from the sample. Images were taken using Canon's Remote Capture program (EOS Utility, Canon Inc., USA). Color parameters were obtained in the Hunter Lab scale using Adobe Photoshop CS8 software (Adobe Systems Inc., San Jose, CA) and then were converted to the standard CIE L^* a^* b^* space using mathematical formulas described by Papadakis, Abdul-Malek, Kamdem, and Yam (2000). The method proposed by Papadakis consists in the acquisition of images by a digital camera and processing of the images to get the color values of the pixels. Graphics software assigns a specific color value to each pixel in the bitmap, providing quantitative information of color distribution which is obtained in terms of L^*, a^* and b^* parameters. The camera was previously calibrated correlating the chromatic coordinates obtained by image analysis with those obtained with a Minolta CM-508 colorimeter (Minolta Co. Ltd., Japan) using a set of matte and opaque colored cards. The degree of opacity of the samples was calculated according to Buera, Farroni, and Agudelo-Laverde (2015):

$$Opacity = L_b^*/L_w^* \quad (6)$$

where L_b^* and L_w^* are the lightness values (L^*) of samples measured over black and white backgrounds, respectively. An opacity value of 1 corresponds to an opaque sample, while lower values correspond to different degrees of translucency. The scattering (S) and absorption (K) coefficients and its ratio (S/K), were obtained from the Kubelka-Munk theory, using the reflectance measurements and mathematical equations described by Judd (1975).

2.3. Statistical analysis

At least two replicate determinations were performed for each trial. A statistical analysis, when necessary, was carried out using *t*-test and differences among compared samples were considered significant at $P > .05$ (interval of confidence of 95%). All statistical analysis and data fitting were performed through GraphPad Version 4 (GraphPad, Software Inc., San Diego, CA, USA).

3. Results and discussion

3.1. Water adsorption of dehydrated alginates-chitosan beads with Prosopis alba gum as wall component

Polyelectrolyte beads containing fish oil were generated by dripping the corresponding emulsion (fish oil stabilized with alginate or alginate-gum) into a calcium chloride solution. The crosslinking of alginate molecules in presence of calcium ions allow the oil entrapment into emulsion-filled gel particles (Scholten, 2018). Wet beads or hydrogels (moisture content 75–80% db.) were further coated through electrostatic adsorption with a chitosan layer and vacuum dehydrated to reduce their water content. Dehydrated A-Ch beads presented a moisture content of 1.31% db., and a mean bead diameter of 1.16 mm, while beads containing the gum (AG-Ch) had a higher water content (3.67% db.) and a higher diameter (1.46 mm). Using scanning electron microscopy, Vasile et al. (2017) found that in dehydrated state, both A-Ch and AG-Ch beads exhibit a multinuclear internal structure where the oil fraction is uniformly dispersed in a solid matrix of Ca-alginate, while in

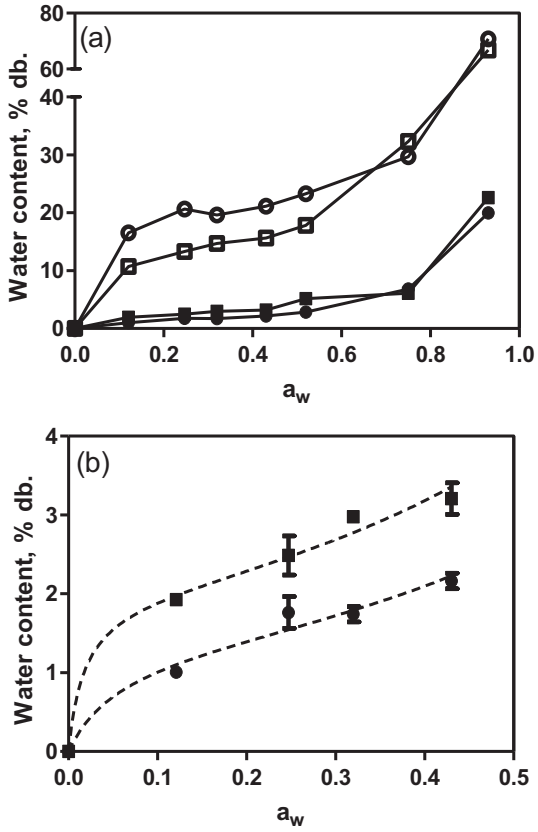

Fig. 1. Water sorption isotherms for alginate-chitosan (●) and alginate-gum-chitosan beads (■) at 25 °C (a), and BET model fitting curves (b) applied for experimental data in the low range of a_w. Capsules containing fish oil (solid symbols) and without oil (empty symbols). Fitting curve (dash lines).

presence of G, an additional physical barrier around oil droplets could be considered based on G interfacial activity (Vasile et al., 2016). Better emulsion stabilizing properties of G helped to explain the smaller size of oil cavities in the multinuclear structure (Vasile et al., 2017).

As was previously reported, G modulates microstructural and functional properties of alginate beads (Vasile et al., 2017). Considering the hygroscopic nature of the studied gum, and the high influence of water on beads structure and encapsulated compounds stability, the analysis of water sorption behavior becomes of fundamental importance to define the appropriate storage conditions of dry formulations. Fig. 1a compares the water sorption isotherms obtained at 25 °C for alginate-chitosan (A-Ch) and alginate/gum-chitosan (AG-Ch) beads employed for the entrapment of a fish oil rich in polyunsaturated fatty acids. In all systems, water sorption isotherms showed a sigmoidal shape with a gradual increase of the water content in the low a_w range and a sharp increase at a_w higher than 0.7. Both the presence of the fish oil and the encapsulating matrix composition (with or without gum), modified the sorption behavior.

Beads containing the oil were markedly less hygroscopic. According to Soazo, Rubiolo, and Verdini (2011), the lower hygroscopicity could be related with a reduction in the availability of surface-active sites for water interactions over the hydrocolloid-oil matrices. Similar results were reported for spray-dried maltodextrin microparticles containing peppermint oil (Adamiec & Kalemba, 2006), where the presence of the lipophilic active led to a reduction in water adsorption in comparison with the respective wall materials.

In beads without oil, a noticeable effect of the encapsulating matrix composition on sorption properties was observed. The presence of the gum as wall component reduced the hygroscopicity of the unfilled beads up to $a_w = 0.5$. Torres, Moreira, Chenlo, and Vázquez (2012) working on polymeric systems also observed less hygroscopicity for higher molecular weight hydrocolloids. Additionally, we observed that when G was present in the alginate-oil emulsion, the concentration of gelling agent ($CaCl_2$) needed for gel formation was lower (Vasile et al., 2017). As consequence, the counter ion salts (NaCl) remaining in the bead structure, could be lower in unfilled AG-Ch than in A-Ch, resulting in a lower hygroscopicity. It is well known that salts, even in small proportions, have a significant effect in low moisture systems increasing solid-water interactions and hence the water content (M. Mazzobre, Longinotti, Corti, & Buera, 2001).

Oppositely, in beads containing the oil, G increased the equilibrium moisture content (M_e) of the beads. In this case, the higher hygroscopicity was related with the oil fraction at bead surface (Vasile et al., 2016). We observed that the surface oil fraction in AG-Ch (1.07 ± 0.04% db.) was significantly lower than in A-Ch (7.87 ± 0.47% db.), evidencing that the presence of G improves the oil retention of the alginate bead network. Entrapment efficiency and oil distribution could be related with emulsifying properties of G. Vasile et al. (2016) reported that G exhibits interfacial properties, forming viscoelastic films at oil/water interface. These authors also observed that G increases the ζ-potential of alginate-fish oil emulsions (−71.2 mV) regard to those emulsions stabilized only with A (−90.6 mV) and explained this effect considering a partial charge neutralization by interaction between positive patches exposed on the protein fraction of G with negatively charged groups present in A (Vasile et al., 2017). Along with the interfacial barrier properties, the electrostatic stabilizing mechanism provided by G, results in more stable emulsions and this was related with the better oil entrapment (lower surface oil fraction) and higher encapsulation efficiencies in beads containing G (98.63%) than in A-Ch beads (89.95%). A lower surface oil fraction leads to a higher proportion of hydrocolloids in the bead surface available to adsorb water.

Above $a_w = 0.5$, the sharp increase of the water sorption could indicate loss of structural integrity of the beads at high water contents and mobility. Velasco et al. (2009) reported similar observations in freeze dried microencapsulates of fish or sunflower oils in matrices of sodium caseinate and D-lactose. They attributed the change in the sorption tendency at high a_w values to a reorganization of the wall capsules molecules and crystallization of small carbohydrates which can take place as viscosity decreases. For this reason, the sorption behavior of the capsules containing oil was evaluated fitting the data up to $a_w < 0.5$, where structural changes are expected to be prevented. The BET model was suitable to describe the experimental data for A-Ch ($R^2 = 0.96$, SEE = 0.09, E = 2.75%) and AG-Ch ($R^2 = 0.97$, SEE = 0.09, E = 1.47%), in the studied a_w range (Fig. 1b). The monolayer water content (M_o), which is an important parameter for storing foods and preventing their deterioration, was 1.37 and 1.96 ± 0.1% db. for A-Ch and AG-Ch, respectively, indicating that in systems containing the gum a higher water content is necessary to saturate the surface active sites. However, the monolayer in AG-Ch beads was reached at a lower a_w value ($a_w = 0.18$) than for A-Ch beads ($a_w = 0.27$) showing that in presence of G, lower storing RH are needed to reach the highest protection of encapsulated oil. The obtained M_o values were lower than those determined by other authors for spray dried encapsulated oils. Botrel et al. (2014) reported values of M_o for fish oil encapsulated by spray drying in whey (M_o = 3.6% db.), whey-maltodextrin (M_o = 2.6% db.) or inulin (M_o = 7.4% db.) matrices. Bonilla, Azuara, Beristain, and Vernon-Carter (2010) also found higher values of M_o for spray dried micro particles containing canola oil and mesquite gum as encapsulating agent (M_o = 5.56% db.). In addition to the composition, the encapsulation method (spray drying, ionic gelation) is known to affect the structure of the beads and therefore the sorption properties.

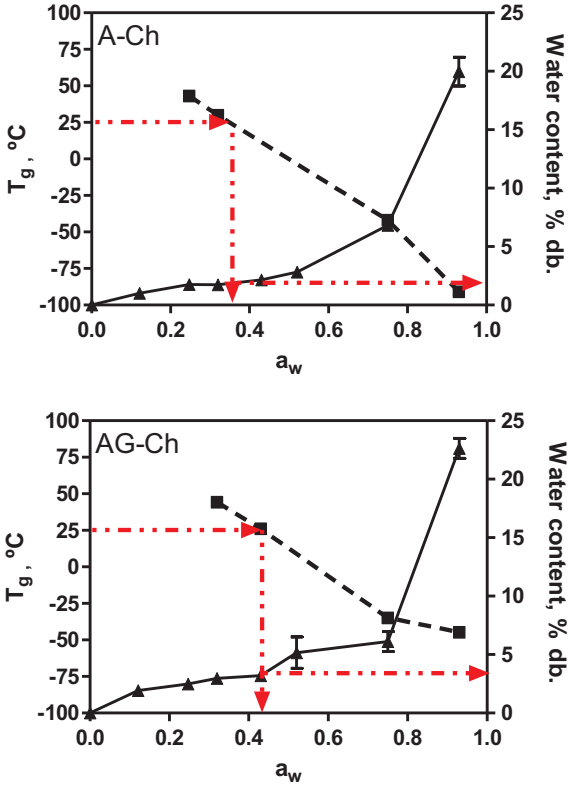

Fig. 2. Glass transition temperatures (■) and water sorption isotherms (▲) of alginate-chitosan (A-Ch) and alginate-gum-chitosan (AG-Ch) capsules containing fish oil at 25 °C. Arrows indicate the critical water activity (CWA) and critical water content (CWC) values evaluated at 25 °C.

3.2. Physical state of dehydrated beads

During drying process, the removal of water from hydrogels leads to an amorphous glassy matrix. In this condition, oxygen diffusion is prevented and oxidative reactions are expected to be delayed (Bell & Hageman, 1994; Escalona-García et al., 2016; Fennema, 2010). However, any increase in temperature or water content may promote the change to rubbery state where diffusion controlled reactions, as lipid oxidation, are accelerated (Slade, Levine, & Reid, 1991). In order to evaluate the impact of the studied gum on the physical state of the polyelectrolyte capsules containing oil, the glass transition temperature (T_g) of the beads equilibrated at different RH was determined by DSC (Fig. 2). As expected, glass transition temperatures decreased with increasing water content in both systems (A-Ch and AG-Ch). T_g values were affected by the encapsulating matrix composition. The impact of the beads composition on water plasticizing of the amorphous solid fraction, was evaluated by the Gordon and Taylor model (Gordon & Taylor, 1952). G addition reduced the glass transition temperature of anhydrous system (T_g) in AG-Ch beads (65 ± 27 °C) respect to A-Ch (138 ± 21 °C). G also reduced the Gordon and Taylor model constant (k_{GT}) for AG-Ch (8.05 ± 3.83) regarding to A-Ch beads (34.21 ± 5.94). Lower T_{gs} values indicate that in presence of G, anhydrous beads need lower temperatures to shift the encapsulates to the supercooled liquid (rubbery) state. It is to be considered also that storage in anhydrous conditions is not recommended for encapsulated oils since it is well known that lipid oxidation could be accelerated in very dry samples (Fennema, 2010; Velasco et al., 2009). A lower k_{GT} indicates that a higher amount of water is needed for achieving a similar T_g reduction respect to control sample. In this sense, the presence of G reduced the susceptibility to water plasticizing effect. In addition, it should be noted that the presence of a single T_g value indicates that hydrocolloids are compatible and interactions between polymeric matrices occur.

Combined T_g-a_w-He diagrams (Fig. 2) were used in order to better understand the effect of G on water/solid interactions and physical state of the encapsulates containing oil, as well as to define the more suitable storage conditions. Critical water activity (CWA) and critical water content (CWC) correspond to those a_w and He limits values, at which glass transition temperature is below the storage temperature. Both the CWA and the CWC were obtained for A-Ch and AG-Ch samples stored at 25 °C from the T_g-a_w-He diagram (Fig. 2).

Encapsulates containing G as wall component showed higher values of CWA and CWC (0.45 and 3.2% db., respectively) compared to capsules without G (CWA = 0.36 and CWC = 2.1% db.). These results indicate that when G is incorporated as wall material, the range of a_w values at which encapsulates are in amorphous state is extended.

3.3. Lipid oxidation related to water activity and T_g

In order to correlate the physical state of encapsulates with their capacity to protect the oil, oxidative damage was evaluated at different RH at 25 °C in A-Ch and AG-Ch beads. Oil extraction and quantification of primary oxidation products were performed after reaching the equilibrium water content in the range 11–95% RH (about 30 days of storage). Fig. 3 shows the peroxide value (PV) determined in A-Ch and AG-Ch beads for selected water activities of the correspondent isotherm. Oxidation was different depending on RH, encapsulating matrix composition and physical state of beads (glassy or rubbery). Capsules without G showed the highest PV over the examined a_w range. Despite alginate-chitosan capsules were widely employed to stabilize different labile compounds by encapsulation, several works recognized their limitations to protect easily oxidizable substances due to porosity, erosion and oxygen permeability (Elnashar et al., 2009; Wang et al., 2013). The lower capacity of the alginate/chitosan capsules to protect the oil against oxidation, was attributed to a lower retention of the oil

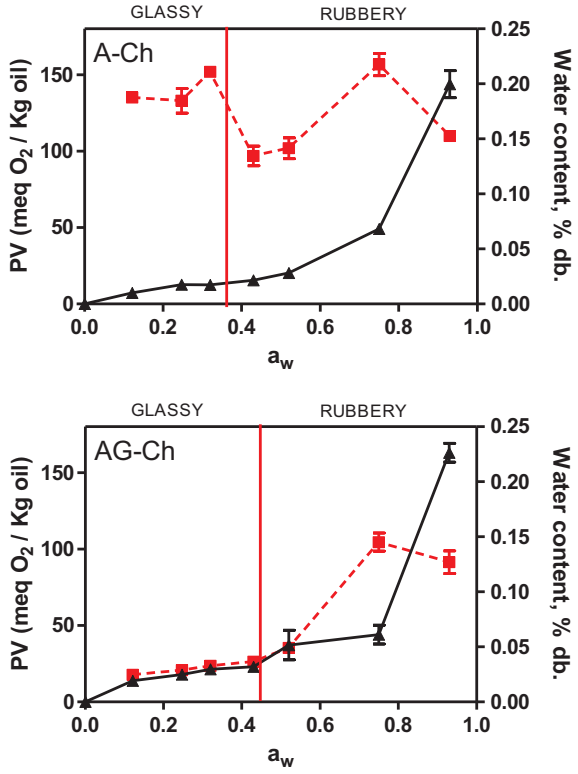

Fig. 3. Oxidative damage determined by Peroxide value, PV (■) and water sorption isotherms (▲) of alginate-chitosan (A-Ch) and alginate-gum-chitosan (AG-Ch) capsules containing fish oil and equilibrated at 25 °C for 40 days. Vertical line indicates the critical water activity value.

within the inner structure (Vasile et al., 2016). Regardless physical state of encapsulating matrix, the oxidative behavior of A-Ch beads was comparable to a bulk oil or continuous lipid systems. As it is well known, lipid oxidation of oils or dehydrated oily foods is highly affected by the water activity. At very dry or very wet environments, lipid oxidation rate is accelerated. However at intermediate moistures, near to monolayer water content, the lipid oxidation reaches a minimum (Labuza, Heidelbaugh, Silver, & Karel, 1971). In this condition, water hydrates metal ions decreasing their catalytic ability, binds hydroperoxides interfering with their decomposition and blocks pores and capillaries for free oxygen diffusion hindering the progress of lipid oxidation (Dobarganes, Márquez Ruiz, & Velasco, 2003).

The lower PV for the oil encapsulated in A-Ch were reached in the range of a_w 0.4–0.5 (Fig. 3), values slightly higher than the correspondent to the monolayer (a_w = 0.27). Similar results were reported by Velasco et al. (2009), who found lower oxidation rates for a physical blend of oil, sodium caseinate and D-lactose, at a_w values higher than the estimated monolayer a_w. These authors also found that near the a_w correspondent to the monolayer, protection of surface oil is maximum while the protection of internal oil fraction is negligible. Hence, in A-Ch beads, at least up to a_w = 0.5, lipid oxidation was probably governed by the surface oil fraction.

In presence of G, encapsulated oil showed lower oxidative damage than A-Ch at each examined water activity. In AG-Ch, lipid oxidation was greatly influenced by the physical state of the encapsulates. In the amorphous state (below CWA value), the encapsulating matrix containing G, showed the highest chemical stability, with very low PV (< 40 meq O_2/kg oil) up to a_w = 0.43. Further increase in PV was coincident with the change of the matrix to the rubbery state where molecular mobility increase due to the plasticizing effect of water on T_g (T_g < $T_{storage}$). Present results showed that oil protection was mainly related with its retention into the inner bead structure. A was previously reported, within the bead matrix G forms intermolecular hydrogen bonds with other polyelectrolytes increasing the tortuosity and promoting the oil retention (Vasile et al., 2017). Also, interfacial activity and viscoelastic film formation of G in oil/water interfaces before drying, suggest that G could provide an effective physical barrier in dehydrated beads that hinder the oil diffusion (Vasile et al., 2016). Low molecular weight sugars in G could act filling the void spaces in the polymeric network favoring the formation of a more compact matrix, limiting simultaneously the oxygen permeability (Vasile et al., 2016). Additionally, the known polyphenol content and the low molecular weight sugars naturally present in G, could contribute to protect the oil (Vasile et al., 2016). According to Elizalde, Herrera, and Buera (2002), during hydration, disruption of hydrogen bonds within the non-crystalline carbohydrate fraction occurs, promoting the release of the entrapped compounds from the dry beads. In this sense, as also state by Ramoneda, Ponce-Cevallos, Buera, and Elizalde (2011) for beta-carotene in amorphous matrices the structural loss of the polyelectrolyte beads could increase the amount of exposed oil to oxygen, favoring the lipid oxidative damage. Natural antioxidant presents in G exerted lower or negligible effect when bead structure was disrupted.

3.4. Appearance properties at different water activities

Water adsorption induced changes in physical and appearance properties of encapsulates containing oil. Regardless encapsulation matrix composition, hydrated samples showed a reduced fluidity with agglomerates formation at highest moisture content. This could be explained considering an extended oxidative polymerization of permeated oil at bead surface with subsequent bridges formation among encapsulates. Polymerization by free radicals is favored on highly unsaturated oils in presence of oxygen, allowing to the formation of solid films (Das, Biswas, Bandyopadhyay, & Pramanik, 2013).

The effect of beads physical changes on chromatic and optical properties of encapsulates was also analyzed in order to establish their relation with water content, structure and protection of the active.

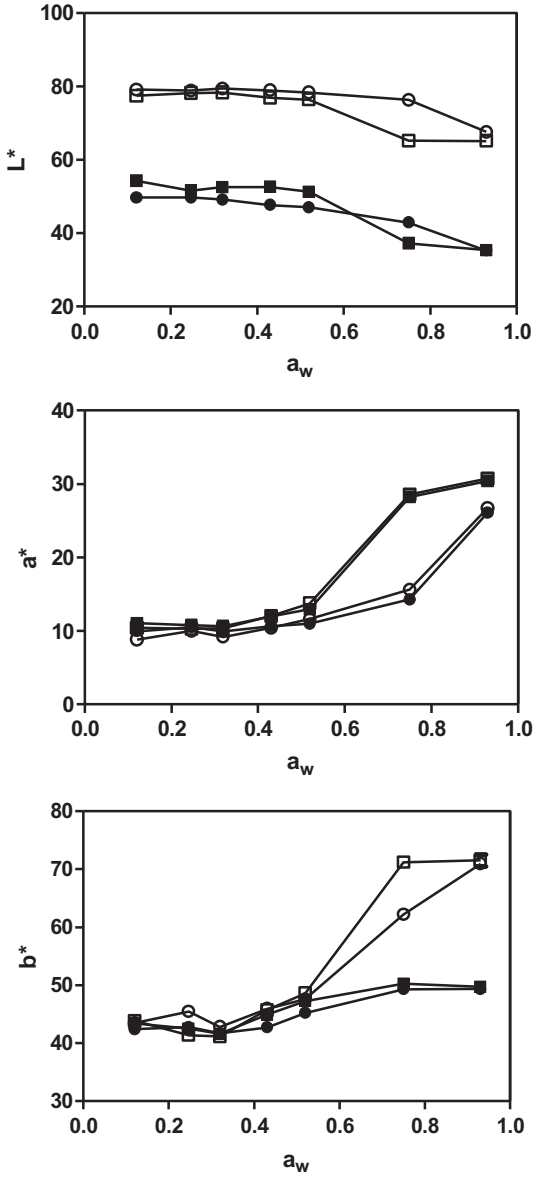

Fig. 4. Chromaticity coordinates at different water activities for alginate-chitosan (●) and alginate-gum-chitosan (■) capsules containing fish oil. White background (empty symbols) and black background (solid symbols).

A more noticeable effect of water adsorption was perceived in the chromatic and optical properties in both systems. In order to evaluate the appearance attributes of encapsulates and relate it with the water content, physical state and oxidative damage, digital image analysis was employed (Papadakis et al., 2000). Fig. 4 shows the variation of CIE L^*, a^* and b^* coordinates, obtained with black and white backgrounds, for A-Ch and AG-Ch systems equilibrated at different water activities.

At higher a_w values, the L^* parameter showed a decrease corresponding to the observed darkening in both systems. Both in AQ and AQ-GAL capsules, L^* varied with the color of the background (black or white) indicating translucency (opacity < 1) of the samples. Translucency was defined as the property of materials to transmit and scatter the light, and ranges from totally transparent to opaque objects (Hutchings, 2011). It was observed that the samples darkened (lower L^*) mainly at a_w values > 0.60, and even more in presence of the gum (Fig. 4). The degree of red (a^*) and yellow (b^*) presented a similar behavior, remaining practically constant and independent of the color of the background up to a_w < 0.6. Above a_w = 0.52 a marked increase

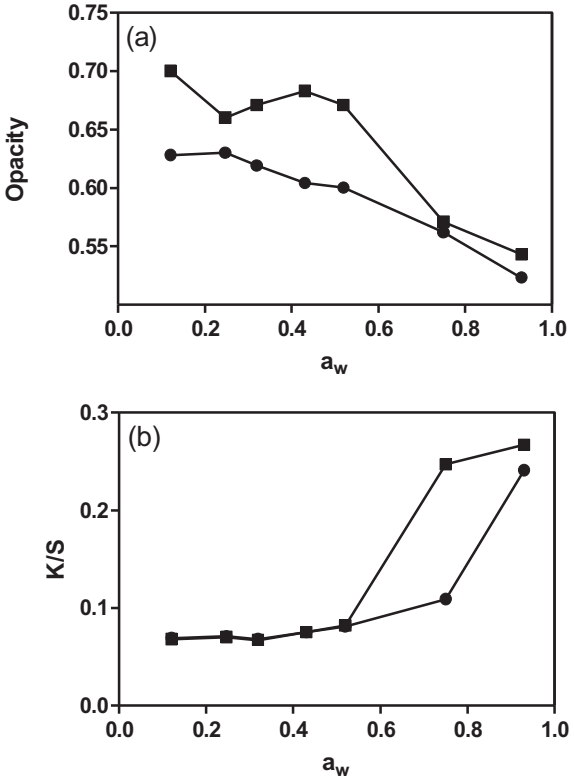

Fig. 5. Opacity (a) and Kubelka-Munk K/S parameters (b) as a function of a_w for alginate-chitosan capsules (●) and alginate- gum-chitosan (■) containing fish oil.

in redness (a^*) and yellowness (b^*) was noticed, being these changes consistent with the brown color visually perceived in those samples. The darkening and color variation of the samples could be related to the formation of polymeric colored substances, consequence of an extensive oil oxidation in conditions of high molecular mobility. It should be noted that the changes in color coordinates occurred sharply and at lower a_w in AG-Ch than in A-Ch. In samples containing G, darkening and browning could also be related with the hydration of pigments (polyphenols and tannins) naturally present in the exuded gum (Vasile et al., 2016) which could explain the higher value of a^* at $a_w = 0.92$ for AG-Ch. At the highest a_w, no differences were observed in L^* and b^* parameters in both systems.

Considering the translucent characteristics of the samples, the opacity and Kubelka-Munk K/S parameters were evaluated as a function of a_w (Fig. 5). In both systems the opacity decreased with increasing a_w, being the values higher for AG-Ch at a_w values lower than 0.75. On the other hand, Fig. 5b shows that no appreciable changes between samples were observed in the K/S coefficient up to $a_w = 0.6$, where a sharp increase was noticed for AG-Ch. According to Hutchings (2011) a higher value of K/S indicates that more light is transmitted than reflected, and hence the material is perceived more transparent. These results are in agreement with opacity measurement, where a reduction in opacity (or increase in transparency) was also verified at high water activities. Similar results were found by Moraga, Talens, Moraga, and Martínez-Navarrete (2011) for lyophilized fruits (banana and apple discs) equilibrated to different RH, in which transparency increased at high water activities. The decrease in opacity (or increase in transparency), has been related to a homogeneous refraction index of the material (Moraga et al., 2011), associated with hydration and filling of cavities with water (Buera et al., 2015). Hollow cavities resulting from water removal during drying create interphases with distinct refractive index and material is perceived opaque. After humidification, water fills the pores of the dried material. As the refractive index of water is closer to the refractive index of the solid than that of air, an increase in the transparency of the material is verified (Buera et al., 2015). In samples containing G, the higher hygroscopicity of the beads probably conduct to verifying transparency at lower water activities than in A-Ch beads. The hydration of AG-Ch could be favored by the hydrophilic nature of the gum. In addition, the higher water content favors the appearance of colored substances due to the formation of oxidized polymers of the oil.

Water sorption and lipid oxidation were critical for the change in optical properties, since the main shifts in chromatic coordinates and K/S parameter occurred at a_w higher than 0.6, while critical T_g values corresponds to a_w 0.45 and 0.36 for AG-Ch and A-Ch, respectively.

4. Conclusion

Prosopis alba exudate gum exerted a noticeable effect on water-solid interactions of alginate-chitosan beads, and on their ability to protect sensitive oils from oxidation. G as wall component increased the hygroscopicity of the beads consequence of a higher oil retention in the inner structure, which leaves more hydrophilic sites available and a higher hydrocolloid fraction exposed at beads surface. The presence of a single T_g value evidenced that components in the beads are compatible. In addition, the presence of the gum as wall component reduced the plasticizing effect of water, extending the range of a_w at which polyelectrolyte beads were glassy. In the amorphous state, encapsulates containing G showed the highest protection against lipid oxidation and chromatic or appearance changes. Chromatic and optical properties of encapsulates were only affected at high water activities, conditions at which an extensive lipid damage was observed. Therefore, the encapsulation of fish oil in alginate-gum-chitosan beads allows obtaining a stable functional ingredient able to be used for the fortification of low moisture content food products such as powdered juices, instant formulae to prepare soups, bakery products, sauces, among others. Present results allow considering *Prosopis alba* exudate gum, as a novel excipient to improve oils protection in alginate beads, with the added benefits of employing an undervalued natural resource.

Acknowledgments

The authors are grateful to Universidad Nacional del Chaco Austral – Argentina (UNCAUS – PI N° 37), Universidad de Buenos Aires – Argentina (UBACYT N° 00443BA), Agencia Nacional de Promoción Científica y Tecnológica – Argentina (ANPCyT, PICT N° 1331), and Consejo Nacional de Investigaciones Científicas y Técnicas – Argentina (CIN-CONICET PDTS 2015 N° 196; PIP N° 00383) for the financial support.

Conflict of interest

The authors of this work declare that they have no conflict of interest.

References

Adamiec, J., & Kalemba, D. (2006). Microencapsulation of peppermint oil during spray drying. In: *Proceedings of the XIVth International Workshop on Bioencapsulation* (pp. 289–292).

Aguilar, K. C., Tello, F., Bierhalz, A. C. K., Garnica Romo, M. G., Martínez Flores, H. E., & Grosso, C. R. F. (2015). Protein adsorption onto alginate-pectin microparticles and films produced by ionic gelation. *Journal of Food Engineering, 154*, 17–24.

Augustin, M., Sanguansri, L., Decker, E., Elias, R., & McClements, D. (2010). Use of encapsulation to inhibit oxidation of lipid ingredients in foods. Oxidation in foods and beverages and antioxidant applications. *Volume 2: Management in different industry sectors*(pp. 479–495).

Bell, L. N., & Hageman, M. J. (1994). Differentiating between the effects of water activity and glass transition dependent mobility on a solid state chemical reaction: Aspartame degradation. *Journal of Agricultural and Food Chemistry, 42*(11), 2398–2401.

Benavides, S., Cortés, P., Parada, J., & Franco, W. (2016). Development of alginate microspheres containing thyme essential oil using ionic gelation. *Food Chemistry, 204*, 77–83.

Beristain, C. I., Azuara, E., & Vernon-Carter, E. J. (2002). Effect of water activity on the stability to oxidation of Spray-dried encapsulated orange peel oil using mesquite gum (*Prosopis juliflora*) as wall material. *Journal of Food Science, 67*(1), 206–211.
Bonilla, E., Azuara, E., Beristain, C., & Vernon-Carter, E. (2010). Predicting suitable storage conditions for spray-dried microcapsules formed with different biopolymer matrices. *Food Hydrocolloids, 24*(6), 633–640.
Botrel, D. A., de Barros Fernandes, R. V., Borges, S. V., & Yoshida, M. I. (2014). Influence of wall matrix systems on the properties of spray-dried microparticles containing fish oil. *Food Research International, 62*, 344–352.
Brunauer, S., Emmett, P. H., & Teller, E. (1938). Adsorption of gases in multimolecular layers. *Journal of the American Chemical Society, 60*(2), 309–319.
Buera, M. P., Farroni, A. E., & Agudelo-Laverde, L. M. (2015). Water and food appearance. In G. F. Gutiérrez-Lopez, L. Alamilla-Beltrán, M.d. P. Buera, J. Welti-Chanes, E. Parada-Arias, & G. V. Barbosa-Cánovas (Eds.). *Water stress in biological, chemical, pharmaceutical and food systems* (pp. 27–40). New York: Springer.
Chen, T., Fowler, A., & Toner, M. (2000). Literature review: supplemented phase diagram of the trehalose-water binary mixture. *Cryobiology, 40*(3), 277–282.
Das, R., Biswas, S., Bandyopadhyay, R., & Pramanik, P. (2013). Polymerized linseed oil coated quartz crystal microbalance for the detection of volatile organic vapours. *Sensors and Actuators B: Chemical, 185*, 293–300.
Dobarganes, M. C., Márquez Ruiz, G., & Velasco, J. (2003). Variables affecting lipid oxidation in dried microencapsulated oils. *grasas y aceites, 54*, 304–314.
Elizalde, B. E., Herrera, M. L., & Buera, M. P. (2002). Retention of β-carotene encapsulated in a trehalose-based matrix as affected by water content and sugar crystallization. *Journal of Food Science, 67*(8), 3039–3045.
Elnashar, M. M., Danial, E. N., & Awad, G. E. (2009). Novel carrier of grafted alginate for covalent immobilization of inulinase. *Industrial & Engineering Chemistry Research, 48*(22), 9781–9785.
Escalona-García, L., Pedroza-Islas, R., Natividad, R., Rodríguez-Huezo, M., Carrillo-Navas, H., & Pérez-Alonso, C. (2016). Oxidation kinetics and thermodynamic analysis of chia oil microencapsulated in a whey protein concentrate-polysaccharide matrix. *Journal of Food Engineering, 175*, 93–103.
Fennema, S. D. K. L. P. O. R. (2010). Quimica de Alimentos de Fennema: Artmed Editora.
Ghorbanzade, T., Jafari, S. M., Akhavan, S., & Hadavi, R. (2017). Nano-encapsulation of fish oil in nano-liposomes and its application in fortification of yogurt. *Food Chemistry, 216*, 146–152.
Gordon, M., & Taylor, J. S. (1952). Ideal copolymers and the second-order transitions of synthetic rubbers. I. non-crystalline copolymers. *Journal of Applied Chemistry, 2*(9), 493–500.
Greenspan, L. (1977). Humidity fixed points of binary saturated aqueous solutions. *Journal of Research of the National Bureau of Standards, 81*(1), 89–96.
Hutchings, J. B. (2011). *Food colour and appearance*. Springer Science & Business Media.
Judd, D. B. (1975). (3rd ed.). *Color in business, science and industry: Vol. 3*Wiley-Interscience.
Labuza, T., Heidelbaugh, N., Silver, M., & Karel, M. (1971). Oxidation at intermediate moisture contents. *Journal of the American Oil Chemists Society, 48*(2), 86–90.
Li, G.-Y., & Li, Y.-J. (2010). Immobilization of Saccharomyces cerevisiae alcohol dehydrogenase on hybrid alginate–chitosan beads. *International Journal of Biological Macromolecules, 47*(1), 21–26.
Mazzobre, M., Longinotti, M., Corti, H., & Buera, M. (2001). Effect of salts on the properties of aqueous sugar systems, in relation to biomaterial stabilization. 1. Water sorption behavior and ice crystallization/melting. *Cryobiology, 43*(3), 199–210.
Mazzobre, M. F., Buera, M. del Pilar, & Chirife, J. (1997). Glass transition and thermal stability of lactase in low-moisture amorphous polymeric matrices. *Biotechnology Progress, 13*(2), 195–199.
Mokhtari, S., Jafari, S. M., & Assadpour, E. (2017). Development of a nutraceutical nano-delivery system through emulsification/internal gelation of alginate. *Food Chemistry, 229*(Supplement C), 286–295.
Moraga, G., Talens, P., Moraga, M., & Martínez-Navarrete, N. (2011). Implication of water activity and glass transition on the mechanical and optical properties of freeze-dried apple and banana slices. *Journal of Food Engineering, 106*(3), 212–219.
Papadakis, S. E., Abdul-Malek, S., Kamdem, R. E., & Yam, K. L. (2000). A versatile and inexpensive technique for measuring color of foods. *Food Technology, 54*(12), 48–51.
Pourashouri, P., Shabanpour, B., Razavi, S. H., Jafari, S. M., Shabani, A., & Aubourg, S. P. (2014). Impact of wall materials on physicochemical properties of microencapsulated fish oil by spray drying. *Food and Bioprocess Technology, 7*(8), 2354–2365.
Ramoneda, X. A., Ponce-Cevallos, P. A., Buera, M. del Pilar, & Elizalde, B. E. (2011). Degradation of beta-carotene in amorphous polymer matrices. Effect of water sorption properties and physical state. *Journal of the Science of Food and Agriculture, 91*(14), 2587–2593.
Rodríguez, J., Martín, M. J., Ruiz, M. A., & Clares, B. (2016). Current encapsulation strategies for bioactive oils: From alimentary to pharmaceutical perspectives. *Food Research International, 83*, 41–59.
Scholten, E. (2018). 4 – Engineered food microstructure for enhanced quality and stability: Case study with emulsions and emulsion-filled gels A2 – Devahastin, Sakamon. *Food microstructure and its relationship with quality and stability* (pp. 59–79). Woodhead Publishing.
Slade, L., Levine, H., & Reid, D. S. (1991). Beyond water activity: Recent advances based on an alternative approach to the assessment of food quality and safety. *Critical Reviews in Food Science & Nutrition, 30*(2–3), 115–360.
Soazo, M., Rubiolo, A., & Verdini, R. (2011). Effect of drying temperature and beeswax content on moisture isotherms of whey protein emulsion film. *Procedia Food Science, 1*, 210–215.
Torres, M. D., Moreira, R., Chenlo, F., & Vázquez, M. J. (2012). Water adsorption isotherms of carboxymethyl cellulose, guar, locust bean, tragacanth and xanthan gums. *Carbohydrate Polymers, 89*(2), 592–598.
Vasile, F. E., Judis, M. A., & Mazzobre, M. F. (2017). Prosopis alba exudate gum as novel excipient for fish oil encapsulation in polyelectrolyte bead system. *Carbohydrate Polymers, 166*, 309–319.
Vasile, F. E., Martinez, M. J., Pizones Ruiz-Henestrosa, V. M., Judis, M. A., & Mazzobre, M. F. (2016). Physicochemical, interfacial and emulsifying properties of a non-conventional exudate gum (Prosopis alba) in comparison with gum arabic. *Food Hydrocolloids, 56*(Supplement C), 245–253.
Vasile, F. E., Romero, A. M., Judis, M. A., & Mazzobre, M. F. (2016). Prosopis alba exudate gum as excipient for improving fish oil stability in alginate–chitosan beads. *Food Chemistry, 190*, 1093–1101.
Velasco, J., Holgado, F., Dobarganes, C., & Márquez-Ruiz, G. (2009). Influence of relative humidity on oxidation of the free and encapsulated oil fractions in freeze-dried microencapsulated oils. *Food Research International, 42*(10), 1492–1500.
Wang, W., Waterhouse, G. I., & Sun-Waterhouse, D. (2013). Co-extrusion encapsulation of canola oil with alginate: effect of quercetin addition to oil core and pectin addition to alginate shell on oil stability. *Food Research International, 54*(1), 837–851.